



Technical Report FP-2010-05

Extended Pierce method for sheet-beam injector design

Stanley Humphries, Ph.D.
Field Precision LLC
Albuquerque, New Mexico U.S.A.
November 2010

1 Introduction

There has been renewed interest in the design of injectors for intense electron beams with non-circular cross sections. The motivating application is the generation of narrow sheet beams to drive novel high-frequency, high-power microwave sources. This report discusses a simple paradigm for designing high-current, sheet-beam guns based on the work of J.R. Pierce¹ He determined electrode shapes to generate an ideal, space-charge-limited beam with the following limitations:

- The result applies to a planar beam of infinite length. In other words, end effects are not addressed.
- The anode is a fixed-potential surface (*i.e.*, a grid), so the effect of an extraction aperture is not included.
- The output beam is non-relativistic (*i.e.*, electron kinetic energy less than 100 keV).

The final design of a practical gun with an aperture requires numerical methods. Nonetheless, the Pierce technique provides a good starting point.

The simulations described in this report show how the Pierce method may be extended to circular and sheet beam injectors, removing the first constraint listed above. The result is a simple prescription for electrode shapes for sheet beam injectors of any aspect ratio. The next section reviews the original Pierce derivation. Section 3 describes calculations with the two-dimensional **Trak** program. They show that a simple modification of the planar beam geometry leads to a high-quality circular-beam injector. Section 4 presents sheet-beam gun designs performed with the three-dimensional **OmniTrak** code. Again, only a small modification of the Pierce electrodes is required to create a high-quality beam.

2 Review of the Pierce method

The Child² law gives the current density and self-consistent potential variation for space-charge-limited electron extraction across an infinite planar gap of width d with applied voltage V_0 . The current density is

$$j_e = \frac{4\epsilon_0}{9} \sqrt{\frac{2e}{m_e}} \frac{V_0^{3/2}}{d^2}. \quad (1)$$

¹J.R. Pierce, *Rectilinear Electron Flow in Beams*, J. Appl. Phys. **11**, 548 (1940).

²CD Child, Phys. Rev. **32**, 492 (1911)

If the cathode is located at $z = 0.0$, then the variation of potential across the gap is

$$\phi(x, y, z) = V_0 (z/d)^{4/3}. \quad (2)$$

Suppose we have a bounded beam with a space-charge-limited flow of electrons in the z direction in the space $x < 0.0$ and vacuum in the space $x \geq 0.0$. The electron flow below the boundary would maintain its properties if we could find shapes for the cathode and anode that produced a variation of electrostatic potential that satisfied two conditions:

- The potential $\phi(0, y, z)$ follows Eq. 2.
- The transverse electric field is zero, or $E_x(0, y, z) = -\partial\phi/\partial x = 0.0$.

The required electrode shapes follow from a solution of the Laplace equation in the upper half plane with the specified boundary conditions. In a two-dimensional planar system, there is a quick method to solve such problems using the properties of complex functions. Take the complex variable u as a linear combination of the real coordinate variables,

$$u = z + jx, \quad (3)$$

where $j = \sqrt{-1}$. An *analytic* function $f(u)$ of a complex variable varies smoothly and has finite derivatives over the region of interest. Analytic functions automatically satisfy the Laplace equation

$$\frac{\partial^2 f}{dz^2} + \frac{\partial^2 f}{dx^2} = 0. \quad (4)$$

The relationship may be verified using the chain rule of partial derivatives.

Equation 4 implies that the real part of any analytic complex function, $\phi = \text{Re}(f)$, is a valid form for the electrostatic potential. The following specific form is useful for the space-charge flow problem:

$$f(u) = V_0 \left(\frac{u}{d}\right)^{4/3} = V_0 \left(\frac{z + jx}{d}\right)^{4/3}. \quad (5)$$

The corresponding electrostatic potential is

$$\phi(x, z) = V_0 \text{Re} \left(\frac{z + jx}{d}\right)^{4/3}. \quad (6)$$

Equation 6 satisfies Eq. 2 along the boundary at $x = 0.0$.

To extract the real part of the potential, it is convenient to express the complex function in the polar coordinates:

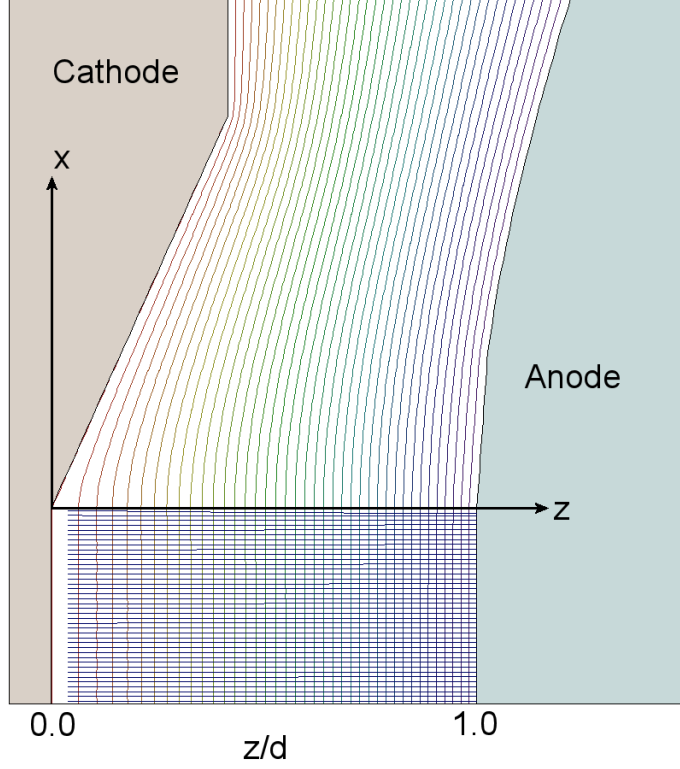


Figure 1: Definition of coordinates for the planar Pierce injector. The system extends an infinite distance out of the page. Calculated model electron orbits and equipotential lines from the **Trak** code.

$$z = \rho \cos \theta, \quad x = \rho \sin \theta. \quad (7)$$

Equation 7 can be written in terms of the complex exponential function

$$e^{j\theta} = \cos \theta + j \sin \theta, \quad (8)$$

as

$$\frac{\phi}{V_0} = \operatorname{Re} \left(\frac{\rho}{d} e^{j\theta} \right)^{4/3} = \left(\frac{\rho}{d} \right)^{4/3} \operatorname{Re}(e^{j4\theta/3}). \quad (9)$$

Where

$$\rho = \sqrt{x^2 + z^2}, \quad \theta = \tan^{-1}(x/z). \quad (10)$$

Applying the chain rule of partial derivatives, Eq. 9 has the property $\partial\phi/\partial x = 0.0$ at $x = 0.0$.

Table 1: Normalized coordinates of the Pierce anode surface.

x/d	z/d
0.00000	1.00000
0.39793	1.02550
0.57746	1.05192
0.72485	1.07916
0.85690	1.10712
0.97985	1.13574
1.09678	1.16494
1.20945	1.19467
1.31897	1.22487
1.42607	1.25551
1.53127	1.28655
1.63493	1.31795
1.73734	1.34969
1.83870	1.38173
1.93919	1.41405
2.00000	1.44000

The shapes of conducting electrodes to generate the field variations may be determined by finding equipotential lines from Eq. 9 at $\phi = 0.0$ and $\phi = V_0$. The cathode lies on the curve

$$4\theta/3 = \pi/2. \quad (11)$$

in the region $x > 0.0$. The equation represents a straight line oriented at 67.5° with respect to the z axis (Fig. 1) The line inclines at angle 22.5° with respect to the electron emission surface. The anode shape is more complex:

$$(\rho/d)^{4/3} \cos(4\theta/3) = 1. \quad (12)$$

Table 1 gives normalized coordinate values determined from a numerical solution.

3 Planar and circular injector calculations

In order to assess the accuracy of computer-generated solutions for sheet-beam injectors, it is essential to quantify the performance of the numerical methods. Accordingly, I set up solutions for the ideal Pierce injector with

both the **Trak** and **OmniTrak** codes. The **Trak** calculation (Fig. 1) described half the injector with symmetry conditions along the lower bound in x . I made the specific choices $d = 1.0$ cm and $V_0 = 20.0$ with a total cathode height of 1.0 cm. I used the *SpaceCharge* mode of **Trak** to exclude small effects of beam-generated magnetic field. The beam was represented by 40 model electrons uniformly distributed in x . The current density predicted by Eq. 1 is 6.590 A/cm².

Twenty iterations were employed to obtain a self-consistent solution for the electrostatic potential variation and electron trajectories. The current density determined by the code was 6.607 A/cm², within 0.2% of the theoretical value. There was less than 0.4% variation over the emission surface. The most sensitive accuracy test is the parallelism of the trajectories. Figure 2a shows the distribution of model electron angles in the vertical direction at the anode plane. The angle was less than 1.0 mrad over the bulk of the beam. The peripheral particles exhibited a small deflection (6.0 mrad) because of electric field averaging over the element width of 0.25 mm. I performed an additional calculation with a flat anode (a plane at $z = d$) to show the effect of the anode shape. The current density rose to 6.72 A/cm² because of the increased electric field with good uniformity over cathode surface. The main effect of the flat anode was on the electron trajectories. The beam had an approximately laminar expansion at the anode with an envelope angle of 13 mrad. Finally, I set up an **OmniTrak** calculation for the geometry of Fig. 1. It represented a 2.5 cm length of injector along y with extrusions used to represent the cathode and anode. The element size was again 0.25 mm. The calculation included 2400 model electrons. The current density determined by the code was 6.53 A/cm², close to the theoretical value. The phase space distribution in the x direction was similar to Fig. 2a. The peak deflection of peripheral electrons was -4.5 mrad.

A practical application of a numerical calculation is the design of a circular-beam injector. The analytic derivation of Sect. 2 is limited to Cartesian coordinates. As a first guess, I converted the electrode profiles of Fig. 1 from extrusions to turnings. In the two-dimensional **Trak** code, the process is simply a matter of interpreting coordinates in the definition of the mesh as z - r values rather than z - x . The flat cathode of radius 0.5 cm had an area 0.7854 cm². The predicted current for an ideal injector is 5.18 A. The numerical solution gave a total current of 4.94 A. The current density varied from 6.39 A/cm² on axis to about 6.15 A/cm² at the edge (Fig. 3). The beam was in compression at the anode with an envelope angle of about -13.5 mrad. A reduction in the angle of the focusing electrode below the Pierce value would simultaneously improve all discrepancies. A smaller angle would raise the current, increase current density on the edge and reduce beam compression. Therefore, I set up a series of runs lowering the angle between the surfaces

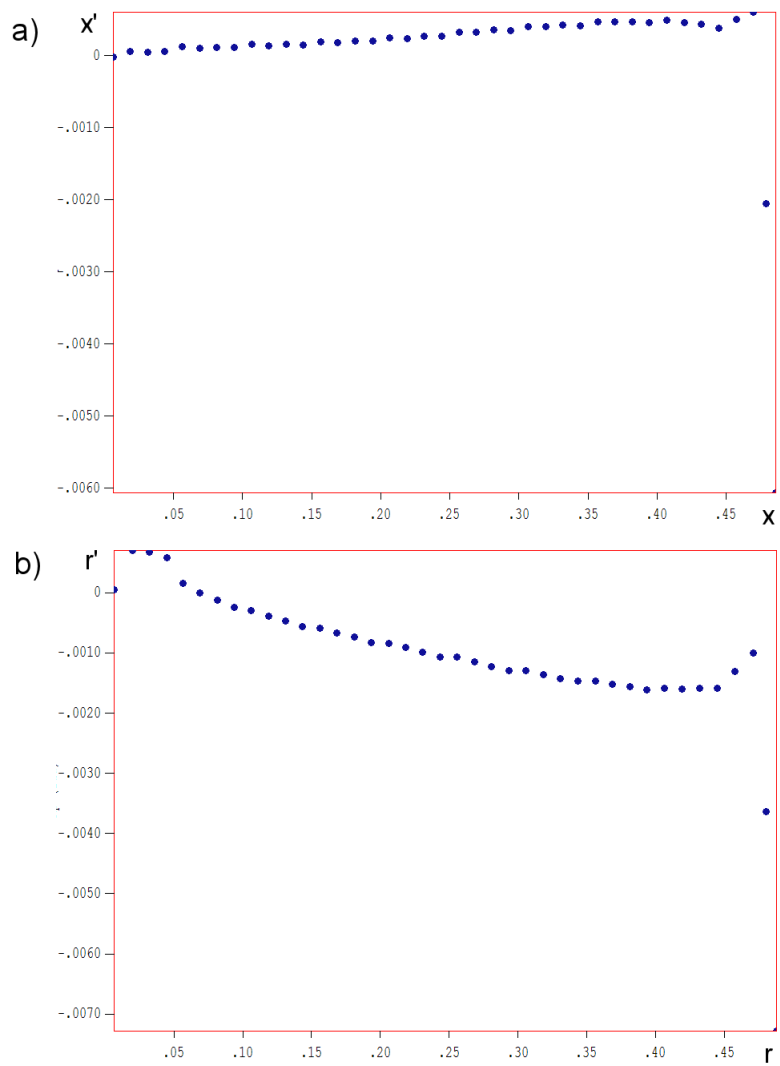


Figure 2: Model electron phase-space distributions at the anode plane ($z = d$). *a*) Planar geometry, plot of x (cm) versus x' (radian). *b*) Optimized cylindrical geometry, plot of r (cm) versus r' (radian).

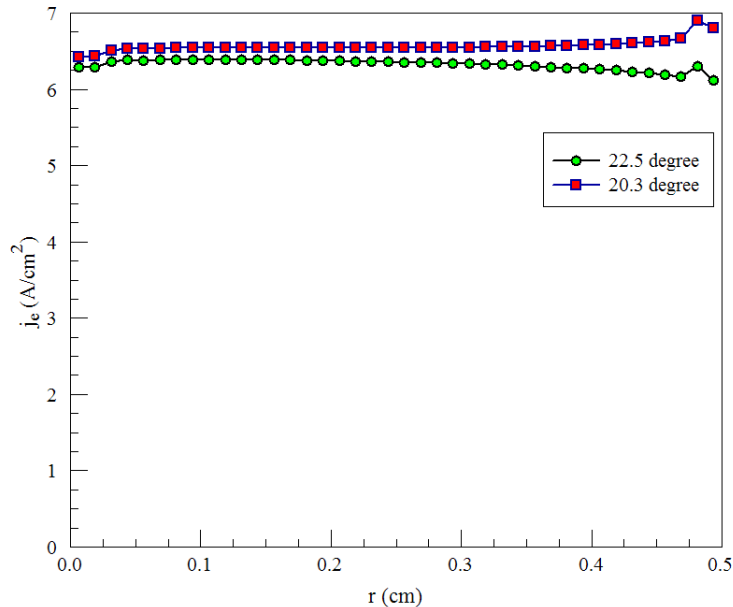


Figure 3: Emitted current-density distribution for a circular injector with cathode radius 0.5 cm for two values of the angle between the emission and focusing electrode surfaces.

of the cathode and focusing electrode. The emitted current reached the theoretical value at an angle of 20.3° . This angle also gave an approximately parallel beam distribution at the anode (Fig. 2b). The current density was about 6.43 A/cm^2 at the center and 6.70 A/cm^2 at the edge (Fig. 3). The gun performance was close to ideal.

4 Sheet-beam design procedure

There are an infinite number of options to design a sheet beam injector. I opted for a simple approach using the Pierce electrode shapes as a guideline. Figure 4a shows the cathode geometry. The emission section was a plane of width W and length L with half circular ends of radius $W/2$. Along the central part, the focusing electrode was an extrusion whose surface intersected the cathode at 22.5° . As shown in Fig. 5, the anode had a flat surface with the same dimensions as the emission surface of the cathode. The flat transitioned to the Pierce profile. The profile was defined an extrusion for $-L/2 \leq x \leq L/2$ and was carried as a turning around the ends. For the demonstration calculation, I used the parameters $d = 1.0 \text{ cm}$, $V_0 = 20.0 \text{ kV}$, $W = 1.0 \text{ cm}$ and $L = 3.0 \text{ cm}$. With a cathode area of 3.784 cm^2 , the predicted total current was 24.94 A .

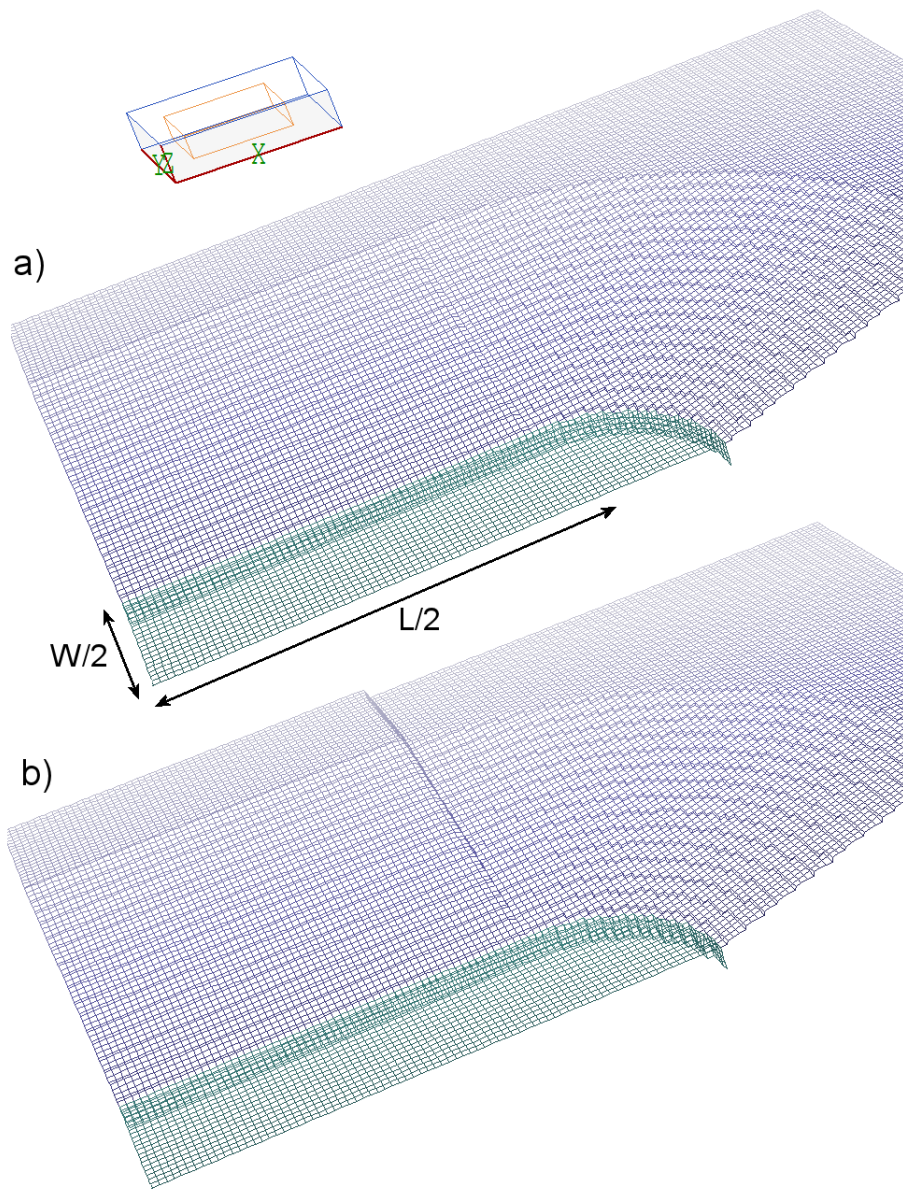


Figure 4: Sheet-beam injector cathode shapes (one-quarter of the assembly). Emission surface in green, focusing electrode in blue. *a)* Initial design. *b)* Improved design.

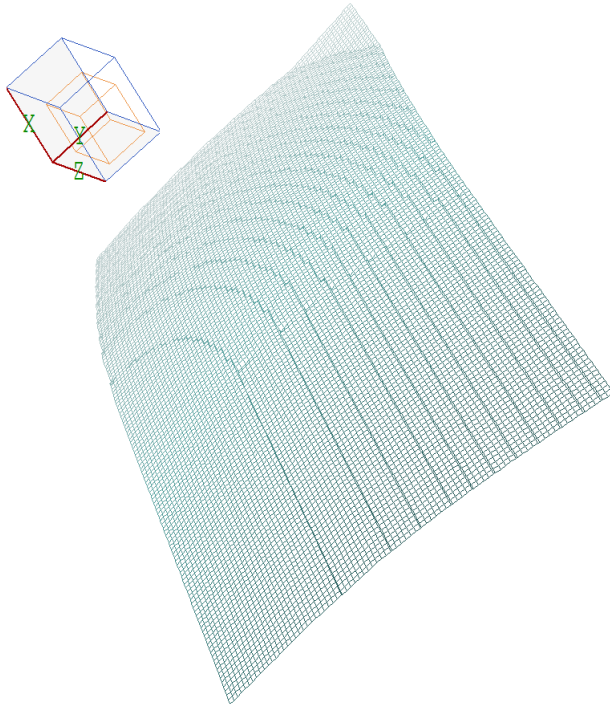


Figure 5: Anode shape (one-quarter of the assembly).

I modeled one-quarter of the assembly, applying symmetry boundaries at $x = 0.0$ cm and $y = 0.0$ cm. As shown in Figs. 4 and 5, the long direction was in x and short direction in y . With an element width of ~ 2.5 mm, the mesh contained 742365 elements. The **OmniTrak** run included 16 cycles that involved tracking 1516 model electrons and determining the space-charge to correct the electrostatic field. The run time was about 10 minutes. The code gave a total emitted current of 24.50 A.

The main imperfection of the design was over-focusing in the end regions. The plot of Fig. 6a illustrates the effect. It shows the x - y coordinates of the model electrons crossing the acceleration gap. The convergence angle is proportional to the displacement (*i.e.*, length of the trace). The deflections on the edge of the central region resulted from electric-field averaging over the element width, the same effect as in the two-dimensional calculations. A non-local displacement is visible in the end regions – the displacement is proportional to the distance from the center. I tried a simple prescription to correct this effect. Motivated by the circular beam results, I used a 22.5° focusing electrode along the straight portions and a 20.3° angle for the turnings around the ends. The geometry is show in Fig. 4b. In this run, the total current was 24.76 A, within 0.07% of the theoretical value. The improvement in electron trajectories is evident in Fig. 6b. An analysis of the distribution

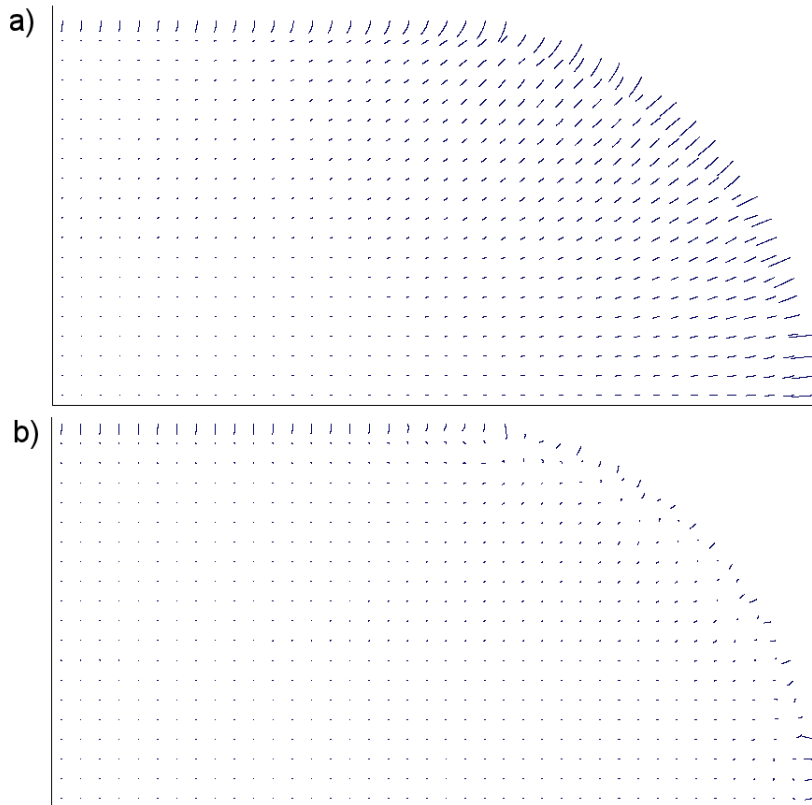


Figure 6: Projected trajectories showing displacements in the $x-y$ plane as electrons cross the acceleration gap. a) 22.5° angle on outer focusing electrode. b) 20.3° angle on outer focusing electrode.

at the anode plane yields average convergence angles of -0.9 mrad in the long direction and -0.7 mrad in the short direction. The angular divergence in both directions was about ± 1.6 mrad.

The final sheet-beam gun design generates a parallel beam with uniform current density. The design is based on a planar cathode and relatively simple electrode shapes. Parts can be fabricated with basic lathe and mill operations. As with planar and circular Pierce-type guns, an anode aperture and its attendant negative lens effect would introduce design issues. In many high-power microwave applications, the goal is to generate a sheet beam with very high aspect ratio (*i.e.*, the length in the long direction is much greater than the height in the short direction). In these applications, the electron beam could be extracted through a one-dimensional aperture and focused by a one-dimensional electrostatic lens. In this case, there are no applied forces in the long direction. Because beam-generated defocusing forces are relatively small, beam expansion in the long direction would be modest.